Analytical Methods

ROYAL SOCIETY OF CHEMISTRY

PAPER

Cite this: *Anal. Methods*, 2020, **12**, 4987

Gas chromatographic-ion mobility spectrometry combined with a multivariate analysis model exploring the characteristic changes of odor components during the processing of black sesame†

Jiang-Shan Zhang,[abc] Zhen-Ling Zhang,*[abc] Meng-Zhen Yan,[abc] Xiu-Min Lin[abc] and Yi-Tian Chen[abc]

Black sesame (*Sesamum indicum* L.) is a Chinese dietary herb that has been widely used in the medical and healthcare fields in China. According to the theory of Traditional Chinese medicine processing, reasonable processing (steaming and drying many times) can increase the tonic effect and reduce the adverse factors generated during long-term use. At present, the processing degree of black sesame is mainly judged based on subjective experience. However, due to the lack of objective and quantitative control indicators, quality fluctuations easily occur. Therefore, for better application, its processing technology needs scientific monitoring methods. Herein a gas chromatography-ion mobility spectrometry (GC-IMS) technique was applied as a monitoring method to differentiate the processed products of black sesame in different processing stages. The response data of volatile components obtained from the samples were processed by the built-in data processing software in the instrument to identify the different components for further principal component analysis (PCA) and orthogonal partial least squares discriminant analysis (OPLS-DA). From fingerprint comparison, 70 differential signal peaks were screened, 32 of which were qualitatively identified, mainly monomers and dimers of 20 compounds. On this basis, the PCA model shows that there was a significant difference between the raw product (S1) and the processed products (H1–9); moreover, there was a certain correlation between the differential changes of samples in different processing stages (H1–9) and the processing times. The OPLS-DA model specifically shows the differential components in the processing with potential characteristics peaks of 41, 105, *n*-nonanal, 2 and ethanol can discriminate whether the BS has undergone the first processed. And the dynamic changes of the three characteristic peaks of 1-hexanol, acetic acid and 107 can determine the specific degree of processing of BS. The research proves that GC-IMS combined with a multivariate analysis model can provide scientific data for identifying the characteristic odor components of black sesame.

Received 29th June 2020
Accepted 2nd September 2020

DOI: 10.1039/d0ay01257b

rsc.li/methods

Introduction

Black sesame (BS) is the dried ripe seed of *Sesamum indicum* L., which is a Chinese medicine with a long history of application since ancient times.[1] It is known for its multiple health benefits including nourishment, hair-blackening and prolonging life in China.[2] Modern research has shown that the medicinal and edible value of BS is closely related to the chemical composition it contains. Sesame oil can provide a variety of essential fatty acids such as α-linolenic acid and linoleic acid required by the body for normal metabolism. And the content of eight essential amino acids in sesame protein is very close to the recommended value of FAO/WHO, accounting for 30% of its total amino acids, which meets the standards of high quality protein. In addition, sesamin and other lignan compounds have various pharmacological activities such as antioxidant, hypolipidemic and liver protection, which can effectively alleviate aging and subhealth status.[3–7] Clinically, BS for chronic deficiency and subhealthy patients with a more chronic course is usually used after steaming and drying, so as to enhance the antioxidant effect and alleviate the health risks caused by the high fat content in raw products, making it easy to assimilate and suitable for long-term use.[8,9] Processing of BS is complex and time-consuming, and improper processing can make it less

[a]*Henan University of Traditional Chinese Medicine, China. E-mail: zhangzl6758@163.com*

[b]*Henan Research Center for Special Processing Technology of Chinese Medicine, China*

[c]*Co-construction Collaborative Innovation Center for Chinese Medicine and Respiratory Diseases by Henan & Education Ministry of P. R. China, China*

† Electronic supplementary information (ESI) available. See DOI: 10.1039/d0ay01257b

effective. Therefore, scientific and effective process control is very important. However, the current chemical and pharmacological research related to the processing action of BS is deficient. This leads to difficulties in obtaining a sufficient scientific basis for the optimization of medicinal processing technologies. With this, the clinical curative quality of the processed products is greatly affected.

BS will produce a rich and characteristic flavor during the entire processing cycle and show obvious differences at different stages, which have great utility value in judging the processing degree. However, it has not been able to effectively apply this approach due to the time-consuming nature of conventional extraction methods and the lack of highly sensitive detection technology. Gas-phase ion mobility spectroscopy[10,11] is a new combination technology that has emerged in recent years. It can analyze trace volatile organic compounds in solid/liquid (with a detection limit as low as the ppbv level) in the headspace without sample preparation. It is very suitable for volatile organic gas and has been widely used in the field of food flavor analysis with gradual extension to the field of traditional Chinese medicine identification.[12–26] In summary, we used GC-IMS to measure the characteristic flavor substances in raw products and processed products at different stages of BS processing, and then, through the built-in fingerprint analysis function of the instrument we calculated variation in the processing of BS. And further, combined with a multivariate analysis model we identified the difference markers. To the best of our knowledge, this is the first report combining GC-IMS and PCA/OPLS to explore changes in volatile components during the processing of BS.

Experimental

Sample preparation

Ten batches of BS samples used in this study were provided by Zhan-Long Wang, a pharmaceutical worker of Guiyuan Tianju Company, Yuzhou, China. The raw product sample (S1) was identified by Professor Zhen-Ling Zhang as the dried ripe seeds of *Sesamum indicum* L. Nine batches of processed samples were prepared from the above corresponding S1 sample according to the traditional Chinese medicine processing technology (steaming and sun-drying nine times) from the intangible cultural heritage in Yuzhou, Henan Province. H1–9 correspond to the samples taken from nine consecutive steaming and drying processes. All the samples were deposited in the Chinese Herbal Medicine Processing Technology Research Lab, Henan University of Traditional Chinese Medicine (Hennan, P. R. China).

Ten portions of powdered samples (each weighing 1 g) of the raw product and processed products of BS were transferred to 20 mL headspace vials. After incubation at 80 °C for 20 min, 500 μL of sample was injected into the FlavourSpec® flavor analyzer for detection and measured three times in parallel.

Apparatus

Measurements were made using a GC-IMS instrument (FlavourSpec®) from the G.A.S. Department of Shandong HaiNeng Science Instrument Co., Ltd. (Shandong, China). The GC column temperature was 60 °C, and the IMS temperature was 45 °C. Nitrogen of 99.999% purity was used as the carrier/drift gas at programmed flow rates as follows: E1 (IMS drift gas) was maintained at 150 mL min^{-1}, E2 (GC carrier gas) was first maintained at 2 mL min^{-1} for 2 min and then increased to 20 mL min^{-1} within 8 min, afterwards it was increased to 150 mL min^{-1} within 10 min and held for 15 min. The retention index (RI) of each compound was calculated using *n*-ketones C_4–C_9 (Sinopharm Chemical Reagent Co., Ltd., Beijing, China) as the external standard. The IMS drift time (Dt) is the time taken for the ions to pass through the drift tube and reach the collector (in milliseconds).

Data analysis

Chemometric processing of the detection data was analysed with the built-in software (LAV, GC-IMS Library Search, Reporter and Gallery plot) of the instrument combined with the PCA and OPLS-DA models. LAV and Reporter were used to view and analyze the original spectrum. GC-IMS Library Search can perform qualitative identification of detected substances according to the built-in NIST database and IMS database. Volatile compounds were identified by comparing RI and Dt of standards in the GC-IMS Library. Gallery Plot can extract the signal of each response compound in the sample and present them in the form of fingerprints for visual and quantitative comparison of the differences between the samples. PCA and OPLS-DA models were used to quantitatively analyze the differences between the samples and screen out the differential markers that have a large difference in the contribution on the basis of spectrum analysis.

Results and discussion

In this study, sensitive GC-IMS technology was proposed to compare S1 and H1–9 according to their volatile components. In Fig. 1, the background of the original spectrum is blue, the abscissa represents the ion drift time after normalization, the red vertical line at 7.9 ms is the reactive ion peak (RIP, normalized time point), and the ordinate represents the GC retention time. Each point on either side of the RIP represents a volatile organic compound (VOC). The color of the points indicates the concentration of the substance: from blue (−0.33 V) to red (0.95 V), the closer the color is to the red, the greater the concentration of the substance; in contrast, the darker the blue, the lower the concentration. The entire spectrum stands for the VOCs of the sample.

S1 was used as a reference to deduct the spectral information of other samples to more intuitively compare the differences between the samples. If the other samples contain the same VOCs as S1, the background after deduction is white, close to red means that the concentration of substances in the corresponding area of the sample is above the reference value, or close to blue means that the concentration is below the reference value. Fig. 2 shows that the spectra of all samples contained many response signals and some of them differed

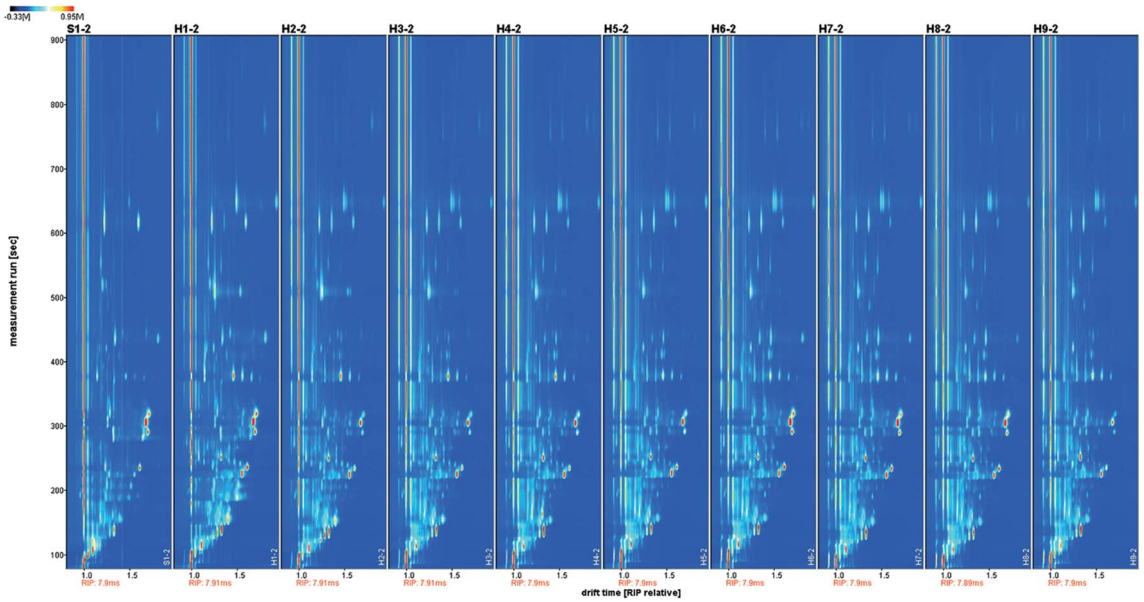

Fig. 1 GC-IMS topographic plots of the samples of S1 and H1–9.

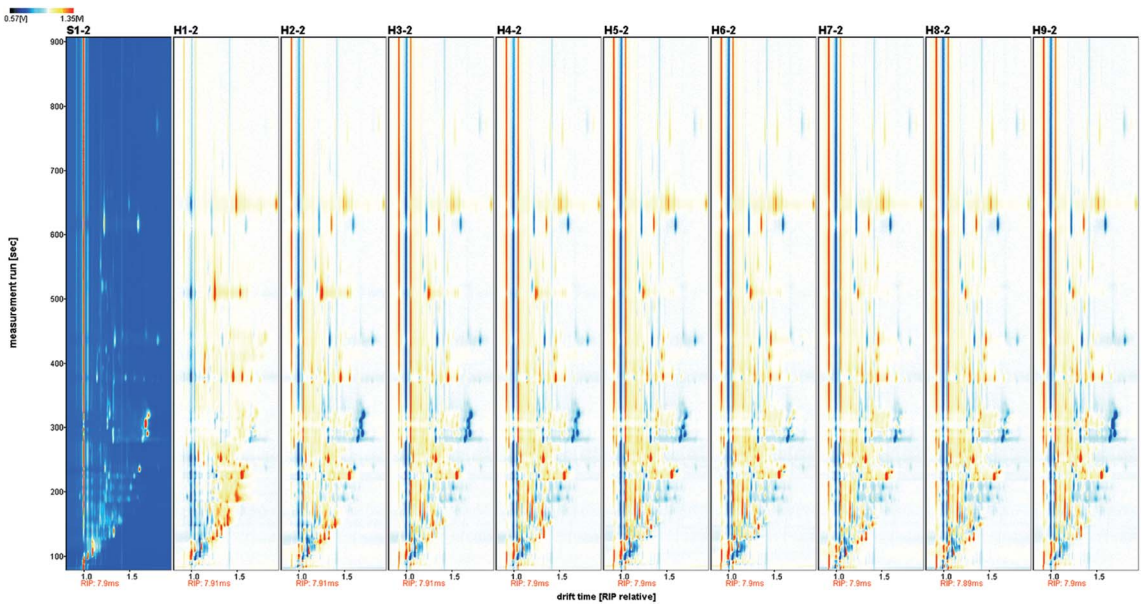

Fig. 2 GC-IMS difference comparison plots of the samples of S1 and H1–9.

significantly in different GC-IMS spectra. The spectra of S1 and H1–9 were clearly different, with the difference between S1 and H1 being the most prominent, while the spectra of H2–8 showed stage changes, H2–5 were more similar, and H6–8 were more similar. In addition, it was evident that the partial response signals varied throughout the entire processing and showed alternating changes of increase and decrease. All response signals were qualitatively identified on the basis of detection (the original qualitative spectrum is attached to the ESI†). Table 1 lists the qualitative results (32 peaks, for 20 compounds) including the compound name, CAS number, molecular formula, molecular weight, RI, retention time and Dt. Some compounds had two response signals due to the presence of monomers and dimers which showed very similar RI, but the Dt of the two were significantly different due to the various molecular weights. It can be seen that BS contains a variety of characteristic VOCs, and there were five main classes of components: alcohols, aldehydes, ketones, acids and esters. Among them, the number of types of aldehydes and esters predominated, alcohols and ketones were the next most numerous, and acids were characterized as only one type. Moreover, 12 of the 20 compounds were present in BS as both monomers and dimers, while the remaining 8 compounds were

Table 1 Qualitative information of the sample

No	Compound	CAS#	Formula	MW	RI	Rt [s]	Dt [RIP relative]	Annotation
1	1-Pentanol	C71410	$C_5H_{12}O$	88.1	759.2	209.062	1.2523	Monomer
2	1-Pentanol	C71410	$C_5H_{12}O$	88.1	758.2	208.43	1.5176	Dimer
3	Butyl acetate	C123864	$C_6H_{12}O_2$	116.2	801.4	236.633	1.2358	Monomer
4	Butyl acetate	C123864	$C_6H_{12}O_2$	116.2	801	236.365	1.6185	Dimer
5	1-Hexanol	C111273	$C_6H_{14}O$	102.2	868.4	285.089	1.3292	Monomer
6	1-Hexanol	C111273	$C_6H_{14}O$	102.2	866.8	283.837	1.6503	Dimer
7	Ethyl valerate	C539822	$C_7H_{14}O_2$	130.2	893.9	306.37	1.2609	Monomer
8	Ethyl valerate	C539822	$C_7H_{14}O_2$	130.2	893.6	306.057	1.6844	Dimer
9	1-Octen-3-one	C4312996	$C_8H_{14}O$	126.2	979.5	408.081	1.2762	
10	Acetophenone	C98862	C_8H_8O	120.2	1061.8	554.846	1.1895	
11	Methyl benzoate	C93583	$C_8H_8O_2$	136.1	1089.7	617.565	1.2271	Monomer
12	Methyl benzoate	C93583	$C_8H_8O_2$	136.1	1089.1	616.048	1.6039	Dimer
13	Ethyl hexanoate	C123660	$C_8H_{16}O_2$	144.2	998.8	435.688	1.3441	Monomer
14	Ethyl hexanoate	C123660	$C_8H_{16}O_2$	144.2	999.1	436.225	1.8179	Dimer
15	Phenylacetaldehyde	C122781	C_8H_8O	120.2	1045	520.27	1.2464	Monomer
16	Phenylacetaldehyde	C122781	C_8H_8O	120.2	1044.2	518.645	1.5374	Dimer
17	*n*-Nonanal	C124196	$C_9H_{18}O$	142.2	1102.6	648.706	1.5003	Monomer
18	*n*-Nonanal	C124196	$C_9H_{18}O$	142.2	1102.3	648.185	1.9467	Dimer
19	Ethanol	C64175	C_2H_6O	46.1	474.3	99.936	1.0474	
20	Acetic acid	C64197	$C_2H_4O_2$	60.1	568.6	125.792	1.058	
21	Furfurol	C98011	$C_5H_4O_2$	96.1	825.4	252.95	1.0812	Monomer
22	Furfurol	C98011	$C_5H_4O_2$	96.1	823.6	251.7	1.33	Dimer
23	Ethyl lactate	C97643	$C_5H_{10}O_3$	118.1	808.4	241.332	1.1408	Monomer
24	Ethyl lactate	C97643	$C_5H_{10}O_3$	118.1	806.4	239.967	1.5385	Dimer
25	Benzaldehyde	C100527	C_7H_6O	106.1	956.9	378.321	1.1463	Monomer
26	Benzaldehyde	C100527	C_7H_6O	106.1	956.9	378.321	1.4659	Dimer
27	(*E*)-2-Octenal	C2548870	$C_8H_{14}O$	126.2	1060.5	552.107	1.3294	
28	2-Heptenal (*E*)	C18829555	$C_7H_{12}O$	112.2	954.4	375.142	1.667	
29	6-Methyl-5-hepten-2-one	C110930	$C_8H_{14}O$	126.2	989.1	421.401	1.1699	
30	(*Z*)-3-Hexen-1-ol	C928961	$C_6H_{12}O$	100.2	847.1	268.684	1.2263	Monomer
31	(*Z*)-3-Hexen-1-ol	C928961	$C_6H_{12}O$	100.2	845	267.18	1.5116	Dimer
32	Ethyl acetate	C141786	$C_4H_8O_2$	88.1	607.9	138.433	1.3315	

present only as monomers, such as 1-octen-3-one, ethanol, acetic acid and (*E*)-2-octenal.

Fig. 3 shows the VOC fingerprint obtained by the Gallery plot plugin integrated from the original GC-IMS spectra of S1 and H1–9. Each row of the fingerprint corresponds to a sample, and each column represents a kind of VOC, the content of which can be indicated by the color of the corresponding square. At the bottom of each column, we mark the signal peaks with a number (there were 117 signal peaks detected, 32 of which were identified and labeled with component names). The

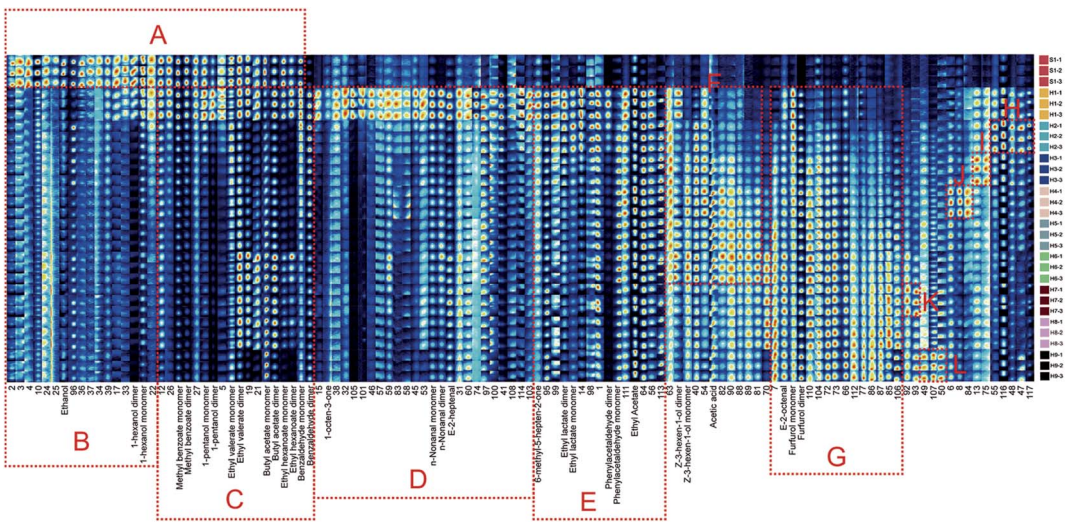

Fig. 3 Fingerprints of all the samples generated by Gallery plot.

change of VOCs in the concoction process can be clearly shown by the difference between the samples in the fingerprint. In Fig. 3, we can find that the VOCs of S1 were mainly concentrated in region A, the VOCs of H1 were mainly concentrated in regions B, C, D and E, and the VOCs of H2–9 were mainly concentrated in regions E, F and G. As a whole, the composition of VOCs in the BS in the processing changed greatly, and the original VOCs reduced while a large number of new VOCs formed. The composition and content of VOCs in H1–9 also varied with the increase in the number of processing times. These changes are likely to be well related to the characteristic flavors developed by BS during the processing. Since the fingerprint of Fig. 3 contains too much information to observe clearly, it was divided into Fig. 4 and 5 for further analysis. The two contained characteristic VOCs belonging to different samples.

In Fig. 4, the difference in the composition of VOCs between S1 and H1 can be clearly observed. As a sample after the initial processing of S1, the composition of VOCs in H1 was significantly changed: a large amount of novel VOCs was generated while some of the original components started to disappear, and only some of them were retained. These dramatic changes in the composition of VOCs were most likely due to the thermal stability of partial components and the Maillard reaction[27] that occurs during the processing. For example, ethanol and hexanol were volatilized easily by heat during the processing, while methyl benzoate, 1-pentanol, ethyl valerate, butyl acetate, ethyl hexanoate and benzaldehyde were not affected much in the initial processing due to their good thermal stability. The heterocyclic compounds such as 1-octen-3-one, nonanal and 2-heptenal (*E*) might derive from the Maillard reaction in the heating process. In addition, some VOCs contained in Fig. 4 were either only in S1 and H1 (such as region B), or the content of both was much greater than that of other samples (such as region D). The identified components of these VOCs can be selected as exclusive markers of S1 or H1.

Fig. 5 shows that the VOCs in the eight regions of E–L were newly generated after processing which were not present in S1. The content of 6-methyl-5-hepten-2-one, ethyl lactate, phenylacetaldehyde and ethyl acetate in region E were decreasing from H1 to H9, probably due to oxidation or decomposition to other products after repeated exposure to heat (steaming) and light (sun drying).[28] The content of (*Z*)-3-hexene-1-ol and acetic acid in the F region first increased and then decreased during the whole processing, which reached the highest in H6. This might be the result of combined effects of decomposition reactions of other components (aldehydes, ketones, esters) and Strecker

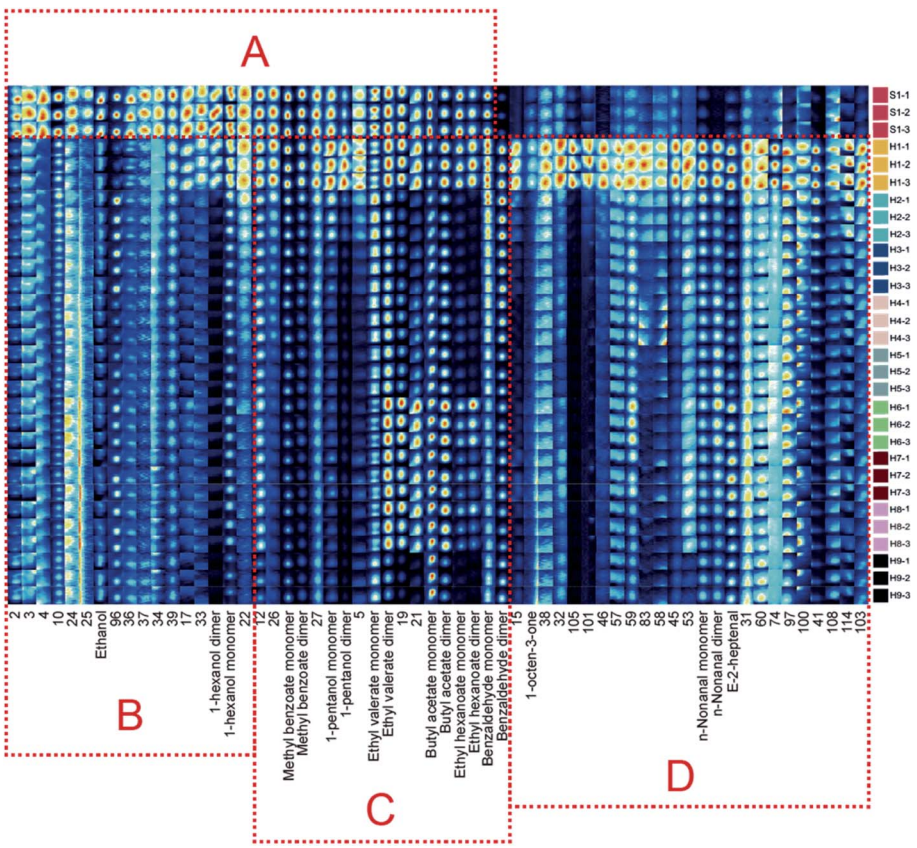

Fig. 4 Characteristic regions in the fingerprint spectra of S1 and H1. (B: 2, 3, 4, 10, 24, 25, ethanol, 96, 36, 37, 34, 39, 17, 33, 1-hexanol, 22) (C: 12, 26, methyl benzoate monomer, methyl benzoate dimer, 27, 1-pentanol monomer, 1-pentanol dimer, 5, ethyl valerate monomer, ethyl valerate dimer, 19, 21, butyl acetate monomer, butyl acetate dimer, ethyl hexanoate monomer, ethyl hexanoate dimer, benzaldehyde monomer, benzaldehyde dimer) (D: 15, 1-octen-3-one, 38, 32, 105, 101, 46, 57, 59, 83, 58, 45, 53, *n*-nonanal monomer, *n*-nonanal dimer, (*E*)-2-heptenal, 31, 60, 74, 97, 100, 41, 108, 114, 103).

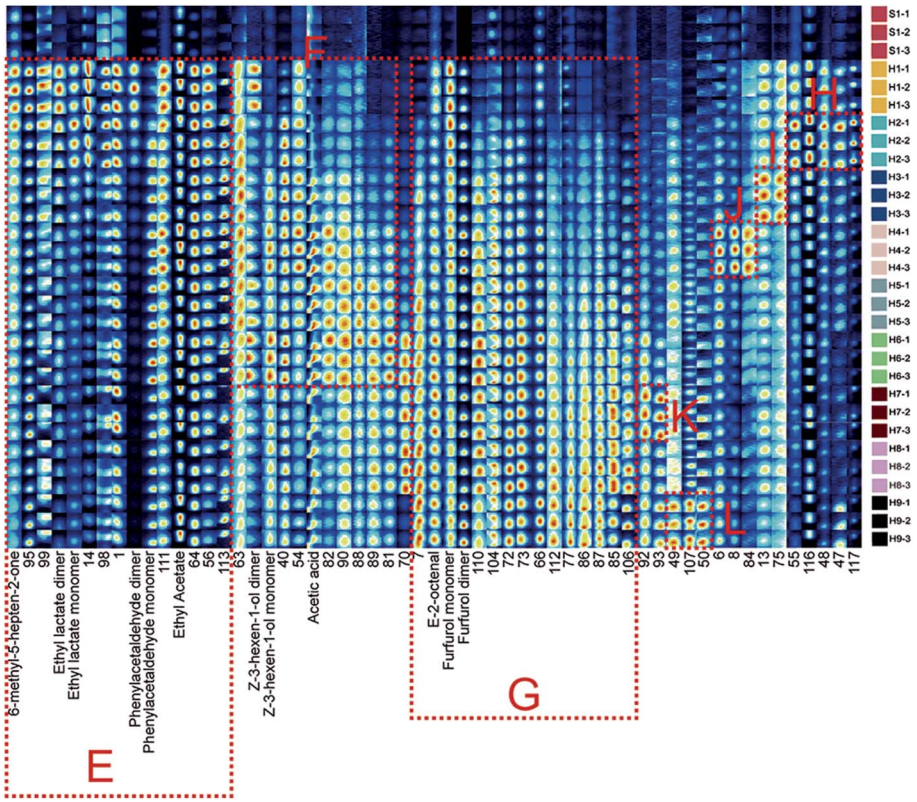

Fig. 5 Characteristic regions in the fingerprint spectra of H2–9. (E: 6-methyl-5-hapten-2-one, 95, 99, ethyl lactate dimer, ethyl lactate monomer, 14, 98, 1, phenylacetaldehyde monomer, 111, ethyl acetate, 64, 56, 113) (F: 63, *z*-3-hexen-1-ol dimer, *z*-3-hexen-1-ol monomer, 40, 54, acetic acid, 82, 90, 88, 89, 81, 70) (G: 7, *e*-2-octenal, furfurol monomer, furfurol dimer, 110, 104, 72, 73, 66, 112, 77, 86, 87, 85, 106) (H: 55, 116, 48, 47, 117) (I: 13, 75) (J: 6, 8, 84) (K: 92, 93) (L: 49, 107, 50).

degradation reactions. The content of 2-octenal and furfural in the G region continued to increase throughout the processing, which reached the highest in H9. Gokmen *et al.*[29] found that the furfural component was an intermediate product of the Maillard reaction, and Meng *et al.*[30] also found an increase in the furfural component during the processing (steaming and sun-drying nine times) of *Rehmanniae Radix Praeparata*. These suggest that the Maillard reaction is likely to be present throughout the processing and is intimately associated with the production of flavour substances. In addition, it can be observed in Fig. 5 that the VOCs contained in H–L regions were components specific to the corresponding processing stages (H2–4, H7, H9), respectively. They may be considered as exclusive markers after identification.

According to the analysis results of the fingerprint (Fig. 3–5), we selected 70 characteristic signal peaks from 8 characteristic regions B, D, F, H, I, J, K, and L, respectively. A PCA model based on their response values was used to further analyze the difference between 10 samples from a quantitative perspective. The total explanatory power of the PCA model for the original variables was 81.88%, which can represent most of the information in the raw data. The analysis results of the PCA model are shown in Fig. 6; the distance of each sphere reflects the similarity between the corresponding samples, and a clear clustering and separation can be found in the distribution of each sample. The 10 groups of samples were mainly divided into three regions, S1, H1 and H2–9, which were very widely spaced. This shows that changes of VOCs in S1 & H1 and H1 & H2 were the most dramatic in the entire processing and there were significant differences between the two. The spacing

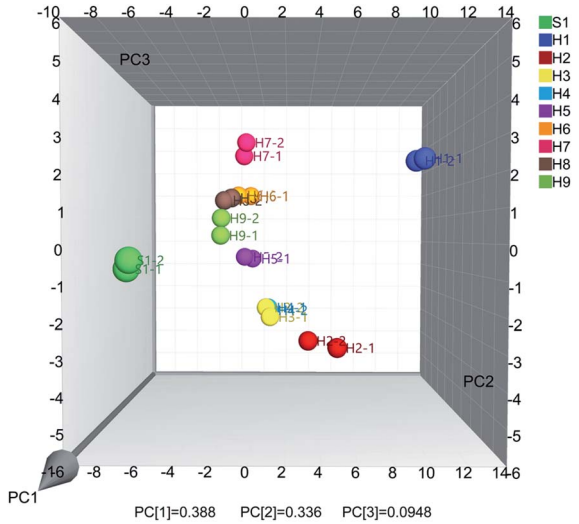

Fig. 6 3D clustering scatter plot of all the samples based on PCA.

between the samples H2–9 was relatively small, but there was still a clear stepwise separation. As in H2–3, H4–5 and H6–7, the separation between the adjacent two was evident. This indicates that the changes of VOCs in the H2–H3, H4–H5 and H6–H7 were more drastic relative to the other stages in H2–H9. In addition, the distribution of H2–5 in PCA exhibited an approximately linear alignment, whereas the distribution of H6–9 showed a distinctly nonlinear alignment. And the spacing of it means that the changes of H6–8 were significantly smaller than that of H6–H7. Thus, S1 and H1–H3 are the stages that have the most impact on the composition of VOCs. The chemical reaction mechanism in this process was the most intense and complex, with a large number of components being produced or lost. This led to significant variability in the samples before and after processing. In contrast, the changes of VOCs in the H4–H5 and H6–H9 were relatively moderate and mainly involved fluctuations in content. However, a small amount of variation in the types of components has caused such fluctuations to show a stepped change.

The OPLS-DA model was established to screen out the differential markers from the above characteristic signal peaks that can effectively distinguish the degree of processing. The S-plot (A) in Fig. 7–9 describes the correlation between the original variables and the discriminant indicators of the model. The positive value interval represents an upward trend and the negative value interval represents a decreasing trend, meanwhile, the closer to the diagonal end of the graph, the greater the difference contribution (VIP). In this study, the VIP value not less than one was used as a screening condition, with red representing VOCs that met the requirements. The histogram (B) in Fig. 7–9 visualized the VIP values of the above eligible VOCs to facilitate further screening for differential markers. Fig. 7 shows the differential marker screening for S1 and H1; there are 11 components representing an increasing trend, most notably 41, 105 and *n*-nonanal monomer; there are 5 components representing a decreasing trend, most notably 2 and ethanol. Fig. 8 shows the differential marker screening for S1 and H1–H9; there are 12 components representing an increasing trend, most notably *n*-nonanal monomer, 6, 10 and acetic acid; there are 9 components representing a decreasing trend, most notably 2 and 1-hexanol. Fig. 9 shows the differential marker screening for H1–H9; there are only 2 components, acetic acid and 107 representing an increasing trend; there are 14 components representing a decreasing trend, most notably 105, 41, *n*-nonanal monomer and 1-hexanol monomer.

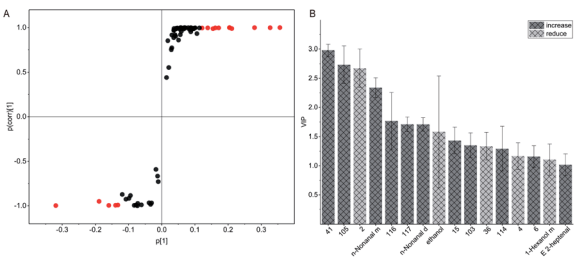

Fig. 7 Screening results of differential markers from S1 and H1.

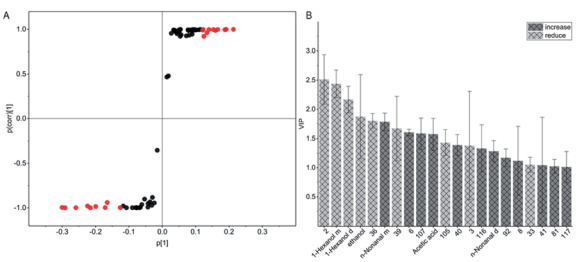

Fig. 8 Screening results of differential markers from S1 and H1–H9.

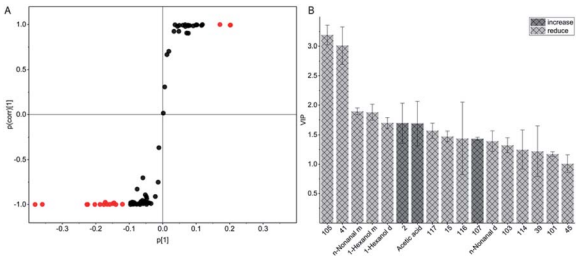

Fig. 9 Screening results of differential markers from H1–H9.

The analysis combined with fingerprinting shows that among the above potential differential markers representing a decreasing trend, 2 was present only in S1, and ethanol was highest in S1. The significant reduction or disappearance of both means that the BS must have gone through processing. 1-Hexanol was only present in S1 and H1, and its disappearance suggests that BS has probably been processed more than twice. Among the above potential differential markers representing an increasing trend, 41, 105 and *n*-nonanal monomer are newly generated components after the first processing. 41 and 105 were found almost exclusively in H1, with the *n*-nonanal monomer being the most abundant in H1. The significant presence of all three at the same time indicates that the BS was likely processed only once. Acetic acid and 107 were absent in both S1 and H1, because acetic acid was only present in H3–9 and 107 was almost only present in H9. The two if present together means that BS has been processed as H9. But if only acetic acid was significantly present, it indicates that BS was in the intermediate stage of processing (H4–H6). Modern research has shown that ethanol[31] can provide energy as a carbohydrate nutrient. It is also an agonist to the GABA receptors and has a depressive effect on the central nervous system. 1-Hexanol is believed to be a component of the odour of freshly mown grass. Its biological mechanism of action also involves the central nervous system, where it is often used clinically as a nicotine antagonist and anesthetic.[32] Nonanal occurs naturally in many citrus fruits, spices and some trees. It has a role as a human metabolite and a plant metabolite, as well as has also been observed in cancer metabolites.[33] Acetic acid has antibacterial properties and the acetyl group derived from it can bind to coenzyme A, which plays a crucial role in the metabolism of carbohydrates and fats.[34] In addition, it has been found to be associated with phenylketonuria, which is an inborn error of

metabolism. The above-mentioned differential markers not only play an important role in the determination of BS processing nodes, but also their biological mechanisms are closely related to human metabolism. It is necessary to properly monitor the dynamics of their content to further investigate their influence on the pharmacological effect of BS.

Conclusions

In this study, we used GC-IMS technology to rapidly detect and identify the composition of VOCs in the raw product and processed products with different degrees of BS. It was found that the original alcohols and esters disappear during the processing of BS, together with the generation of a large number of aldehydes and ketones, which were constantly changing. The content of most of the alcohols, ketones and esters among the identified components showed a positive or negative correlation with the number of processing times, while the changes in acids, partial esters and aldehydes were relatively complex. Based on the PCA analysis, it can be concluded that the presence of the Maillard reaction during the steaming process caused a dramatic change in the type of VOCs in the initial stage (S1 and H1–H3). It is a critical factor in the formation of characteristic flavor substances of BS. Besides, continuous steaming and sun drying also make the content of VOCs continuously change throughout the process. This is an important reason why the composition of flavouring substances in BS tends to be stable. According to the OPLS-DA analysis, the dynamic changes of differential markers such as ethanol, *n*-nonanal, 1-hexanol and acetic acid can determine the extent of processing of BS. The results were consistent with the analysis of proprietary markers in fingerprints. This further proves the feasibility of combining GC-IMS and multivariate analytical models for the analysis of complex chemical constituents in natural products.

Conflicts of interest

The authors declare that there are no conflicts of interest.

Abbreviations

BS	*Sesamum indicum* L
S1	Raw product sample
H1	First processed sample
H9	Final processed sample
H1–9	1st to 9th processed samples
PCA	Principal component analysis
OPLS-DA	Orthogonal partial least squares discriminant analysis

Acknowledgements

The authors gratefully acknowledge the financial support of the industry special project for the public welfare of State Administration of Traditional Chinese Medicine of China (00104296) and the graduate student research innovation project of Henan University of Traditional Chinese Medicine (2019KYCX020).

References

1 Chinese Pharmacopoeia Commission, *Pharmacopoeia of the People's Republic of China*, China Medical Science Press, Beijing, 2020, vol. 1, p. 359.
2 F. Shan, L. Q. Huang, J. Guo and M. Chen, *Chin. Bull. Life Sci.*, 2015, **27**, 1061–1069.
3 T. O. Fasuan, T. O. Omobuwajo and S. O. Gbadamosi, *J. Food Process. Preserv.*, 2018, **42**, e13341.
4 J. N. Huang, Z. L. Ai and X. Lu, *Sci. Technol. Food Ind.*, 2012, **33**, 398–401.
5 P. K. Kancharla and N. Arumugam, *J. Am. Oil Chem. Soc.*, 2020, **97**, 475–483.
6 C. M. Kumar, U. V. Sathisha, S. Dharmesh, A. G. A. Rao and S. A. Singh, *Biochimie*, 2011, **93**, 562–569.
7 A. F. Majdalawieh, M. Massri and G. K. Nasrallah, *Eur. J. Pharmacol.*, 2017, **815**, 512–521.
8 S. T. Yan, H. Fan, R. L. Li, L. P. Wang, W. J. Luo, F. Gao, L. Chen and P. F. Wei, *China Pharm.*, 2020, **23**, 136–141.
9 J. Liu, Y. L. Zhang, Y. N. Mu and B. B. Zhang, *Western Journal of Traditional Chinese Medicine*, 2018, **31**, 27–30.
10 S. Armenta, M. Alcala and M. Blanco, *Anal. Chim. Acta*, 2011, **703**, 114–123.
11 S. Q. Wang, H. T. Chen and B. G. Sun, *Food Chem.*, 2020, **315**, 126158.
12 G. Cao, Q. Y. Shou, Q. L. Li, J. P. Jiang and X. C. Chen, *J. Sep. Sci.*, 2014, **37**, 3090–3093.
13 Q. L. Li, R. Q. Li, G. Cao, X. Wu, G. M. Yang, B. C. Cai, B. Cheng and W. M. Mao, *J. Sep. Sci.*, 2015, **38**, 3205–3208.
14 M. Tzschoppe, H. Haase, M. Hohnisch, D. Jaros and H. Rohm, *Food Control*, 2016, **64**, 17–21.
15 N. Gerhardt, M. Birkenmeier, S. Schwolow, S. Rohn and P. Weller, *Anal. Chem.*, 2018, **90**, 1777–1785.
16 Z. Y. Yuan, H. Y. Qu, M. Z. Xie, G. Zeng, H. Y. Huang, F. Ren and N. H. Chen, *Anal Methods*, 2019, **11**, 530–536.
17 M. D. Contreras, N. Jurado-Campos, L. Arce and N. Arroyo-Manzanares, *Food Chem.*, 2019, **288**, 315–324.
18 X. Sun, D. Y. Gu, Q. B. Fu, L. Gao, C. Shi, R. T. Zhang and X. G. Qiao, *Food Sci. Nutr.*, 2019, **7**, 1387–1395.
19 S. L. Jia, Y. Li, S. Zhuang, X. H. Sun, L. T. Zhang, J. Shi, H. Hong and Y. K. Luo, *Food Microbiol.*, 2019, **84**, 103248.
20 T. Chen, X. P. Qi, M. J. Chen and B. Chen, *J. Anal. Methods Chem.*, 2019, **2019**, 3163204.
21 M. Hernandez-Mesa, D. Ropartz, A. M. Garcia-Campana, H. Rogniaux, G. Dervilly-Pinel and B. Le Bizec, *Molecules*, 2019, **24**, 2706.
22 L. L. Tian, Y. Y. Zeng, X. Q. Zheng, Y. H. Chiu and T. Liu, *Food Anal Method*, 2019, **12**, 2282–2292.
23 E. Budzynska, S. Sielemann, J. Puton and A. L. R. M. Surminski, *Talanta*, 2020, **209**, 120594.
24 M. D. Contreras, L. Aparicio and L. Arce, *LWT–Food Sci. Technol.*, 2020, **120**, 108897.
25 H. M. Li, D. Q. Jiang, W. L. Liu, Y. Q. Yang, Y. S. Zhang, C. W. Jin and S. Y. Sun, *Food Res. Int.*, 2020, **128**, 108801.

26 W. S. Lv, T. Lin, Z. Y. Ren, Y. Q. Jiang, J. Zhang, F. J. Bi, L. H. Gu, H. C. Hou and J. N. He, *Food Res. Int.*, 2020, **131**, 108985.
27 Y. Q. Zhou, F. Y. He, Y. T. Yang, J. L. Shi, K. W. Deng, Y. Tang and W. L. Liu, *Chin. Tradit. Herb. Drugs*, 2014, **45**, 125–130.
28 I. H. Cho, S. Y. Kim, H. K. Choi and Y. S. Kim, *J. Agric. Food Chem.*, 2006, **54**, 6332–6335.
29 A. Hamzalioglu and V. Gokmen, *Food Chem.*, 2018, **240**, 354–360.
30 X. L. Meng, J. N. Ma, S. S. Zhang, K. Li, F. F. Xue, J. Zhang, Z. C. Yuan, Y. F. Tian and M. F. Wang, *Chin. Tradit. Herb. Drugs*, 2016, **47**, 752–759.
31 *National Center for Biotechnology Information*, https://pubchem.ncbi.nlm.nih.gov/compound/Ethanol, accessed August 2020.
32 *National Center for Biotechnology Information*, https://pubchem.ncbi.nlm.nih.gov/compound/1-Hexanol, accessed August 2020.
33 *National Center for Biotechnology Information*, https://pubchem.ncbi.nlm.nih.gov/compound/Nonanal, accessed August 2020.
34 *National Center for Biotechnology Information*, https://pubchem.ncbi.nlm.nih.gov/compound/Acetic-acid, accessed August 2020.